AIP Advances

Faraday-cage-assisted etching of suspended gallium nitride nanostructures

Cite as: AIP Advances **10**, 055319 (2020); https://doi.org/10.1063/5.0007947
Submitted: 18 March 2020 . Accepted: 28 April 2020 . Published Online: 21 May 2020

Geraint P. Gough, Angela D. Sobiesierski, Saleem Shabbir, Stuart Thomas, Daryl M. Beggs, Robert A. Taylor, and Anthony J. Bennett

COLLECTIONS

Paper published as part of the special topic on Chemical Physics, Energy, Fluids and Plasmas, Materials Science and Mathematical Physics

View Online

Export Citation

CrossMark

ARTICLES YOU MAY BE INTERESTED IN

Baking and plasma pretreatment of sapphire surfaces as a way to facilitate the epitaxial plasma-enhanced atomic layer deposition of GaN thin films
Applied Physics Letters **116**, 211601 (2020); https://doi.org/10.1063/5.0003021

Development of microLED
Applied Physics Letters **116**, 100502 (2020); https://doi.org/10.1063/1.5145201

Jet propulsion by microwave air plasma in the atmosphere
AIP Advances **10**, 055002 (2020); https://doi.org/10.1063/5.0005814

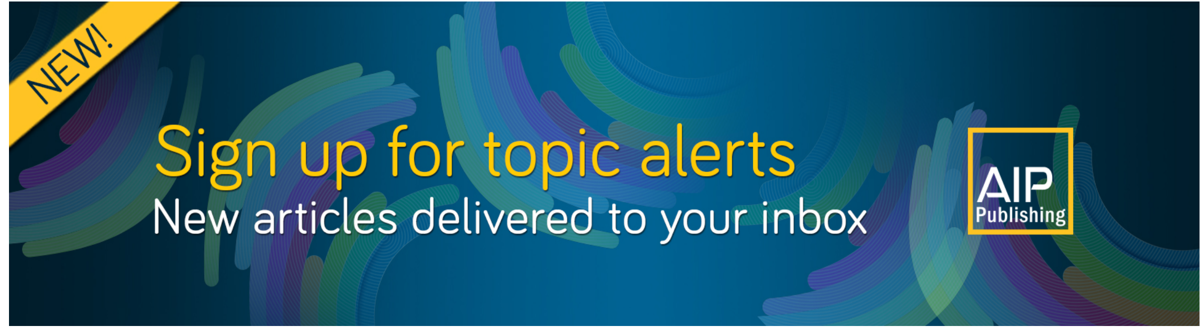

© 2020 Author(s).

Faraday-cage-assisted etching of suspended gallium nitride nanostructures

Cite as: AIP Advances 10, 055319 (2020); doi: 10.1063/5.0007947
Submitted: 18 March 2020 • Accepted: 28 April 2020 •
Published Online: 21 May 2020

View Online Export Citation CrossMark

Geraint P. Gough,[1,2] Angela D. Sobiesierski,[3] Saleem Shabbir,[3] Stuart Thomas,[3] Daryl M. Beggs,[1] Robert A. Taylor,[4] and Anthony J. Bennett[5,a)]

AFFILIATIONS

[1] School of Physics and Astronomy, Cardiff University, Queen's Buildings, Cardiff CF24 3AA, United Kingdom
[2] The Bristol Centre for Nanoscience and Quantum Information, 5 Tyndall Ave., Bristol BS8, United Kingdom
[3] Institute for Compound Semiconductors, Cardiff University, Queen's Buildings, Cardiff CF24 3AA, United Kingdom
[4] Clarendon Laboratory, Department of Physics, University of Oxford, Parks Road, Oxford OX1 3PU, United Kingdom
[5] School of Engineering, Cardiff University, Queen's Buildings, Cardiff CF24 3AA, United Kingdom

[a)] **Author to whom correspondence should be addressed:** BennettA19@cardiff.ac.uk

ABSTRACT

We have developed an inductively coupled plasma etching technique using a Faraday cage to create suspended gallium-nitride devices in a single step. The angle of the Faraday cage, gas mix, and chamber condition define the angle of the etch and the cross-sectional profile, which can feature undercut angles of up to 45°. We fabricate singly- and doubly-clamped cantilevers of a triangular cross section and show that they can support single optical modes in the telecom C-band.

© 2020 Author(s). All article content, except where otherwise noted, is licensed under a Creative Commons Attribution (CC BY) license (http://creativecommons.org/licenses/by/4.0/). https://doi.org/10.1063/5.0007947

Modern semiconductor nanofabrication techniques can be used to create three-dimensional device geometries that support integrated photonic, electronic, and mechanical functionalities. In silicon, the Bosch process can create devices with deep vertical sidewalls with an anisotropic etch or undercut surface layers using an isotropic etch. These etches can create acceleration sensors,[1] high-quality resonators that can be cooled to their vibrational ground state,[2] and advanced quantum photonic processors[3] on the silicon platform. Alternatively, in a direct bandgap AlAs/GaAs system, a strong hydrofluoric acid etch selectivity exists, which enables the creation of suspended photonic crystals, waveguides, and mechanical resonators[4,5] containing integrated light sources in the near infrared.[6] An open challenge is creating similar devices in wide-bandgap semiconductors that may operate in the visible spectral range. Recently, suspended 3D nanocavities have been fabricated in glass using angled focused ions beams,[7] but this can cause damage to the host material through ion implantation.[8] A promising alternative is the use of angled dry etching.[9–11] Suspended beams have been fabricated in diamonds by placing the sample inside a Faraday cage in an inductively coupled plasma (ICP) chamber to undercut a lithographically defined resist pattern.[12] The Faraday cage deflects the ions, causing them to impact on the sample at steep angles, removing the material beneath a masked area. Etches within Faraday cages of a triangular cross section have been used to create suspended devices with a triangular cross section in diamonds, quartz, or silicon.[13]

Gallium nitride (GaN) is a commercially important semiconductor with widespread use in solid state lighting, blue lasers, and high speed and high power electronics. It has a wide direct bandgap of 3.4 eV, a refractive index of 2.3 at 1550 nm, a large Pockel's electro-optic effect and low absorption across the visible and near-IR part of the spectrum. In addition, heterostructures can be designed with light sources from the ultraviolet to the infrared based on quantum wells,[14] quantum dots,[15] and color centers.[16] These properties make GaN a promising material for integrated photonics across a wide spectral range.[17]

Suspended photonic devices in GaN have been fabricated using multi-step reactive ion etching (RIE) or inductively coupled plasma (ICP) processes, typically resulting in near-vertical sidewalls.[18,19] First, a vertical etch is used to define a pattern in the GaN surface

© Author(s) 2020

layer. Then, a sacrificial layer beneath the surface can be removed, for example, by photo-electrochemical etching of the InGaN sacrificial layer.[15,20] Alternatively, for GaN layers grown on a silicon substrate, it is possible to selectively etch the silicon, leaving a suspended GaN membrane.[21,22]

Here, we demonstrate a single step Faraday cage-assisted etch to create high contrast waveguides with a triangular cross section. We report the conditions, cage design, and processes to create free standing devices in GaN in a single step. Such technology could be used to create GaN micro-electro-mechanical systems (MEMS) or suspended photonic crystal lasers in this technologically important material.

Figure 1 illustrates the concept of the Faraday cage assisted etch. Figure 1(a) shows a cross section of the cage within the ICP chamber, containing a cage with a triangular cross-section and a sample located at the center. Ions from the plasma are directed downward by the field between the anode and cathode. As these ions are incident on the mesh covering the walls of the cage, they are deflected from the vertical direction, being incident on the sample at an angle θ relative to the normal. The resulting etch undercuts the resist to create the characteristic cross-sectional profile, as shown in Fig. 1(b). We expect that region I [shown in Fig. 1(b)] is bombarded with ions from the left and right sides of the cage and so is etched to a depth of $2d$. However, region II is only bombarded with ions from the left and is thus etched to a depth of d, as shown. Region III is protected by a hard resist, such as a layer of nickel, which can be subsequently removed by acid. When the etch is dominated by the mechanical action of the ion impact, we expect the etch angle θ to be determined by the trajectory of ions deflected by the mesh. The angle in the lower part of the etch profile, $\phi = \tan^{-1}((3\tan\theta)^{-1})$, is plotted as a function of θ, as shown in Fig. 1(c).

The cage we use is shown in panel (d) of Fig. 1. It has a cross-sectional profile of an equilateral triangle, and a length of 70 mm, covered with a square pattern mesh of 0.25 mm diameter wire and 1.00 mm apertures. The housing of the cage and mesh consists of the aluminum 5056 alloy, as is used in construction of the etch chamber walls, to prevent contamination of the system.

We show in Fig. 1(e) a cross-sectional scanning electron microscope (SEM) image of GaN etched to a depth $2d = 1.56$ μm using the cage described above. The profile of the etch is similar to the expected form with $\theta = 30°$. In practice, deviations from the profile, as shown in Fig. 1(b), result from etching of the hard mask at its edges during long processes, which will tend to reduce the angle θ observed. In addition, as the etch progresses, there will be edge effects deflecting the angle of the ions as they pass the edge of the Ni metal mask. Finally, this model assumes that the mechanical part of the etch is dominant and does not include the effect of the chemical part of the etch process due to the chlorine ions. A detailed analysis of the deflection of ions in Faraday cage-ICP etching is given by Latawiec *et al.*[13]

From the experiment, we have noted that the angle of the etch θ achieved is always less than the angle the cage walls make to the cathode, suggesting the ions do not travel into the cage at right angles to the mesh. We have also noted that cages with a top support [shown in Fig. 1(a)] achieve a higher angle θ, which we attribute to the prevention of vertical ion ingress through the cage apex. We have also noted the importance of minimizing the presence of structured metal fixings on the cage. These fixings, such as the screws

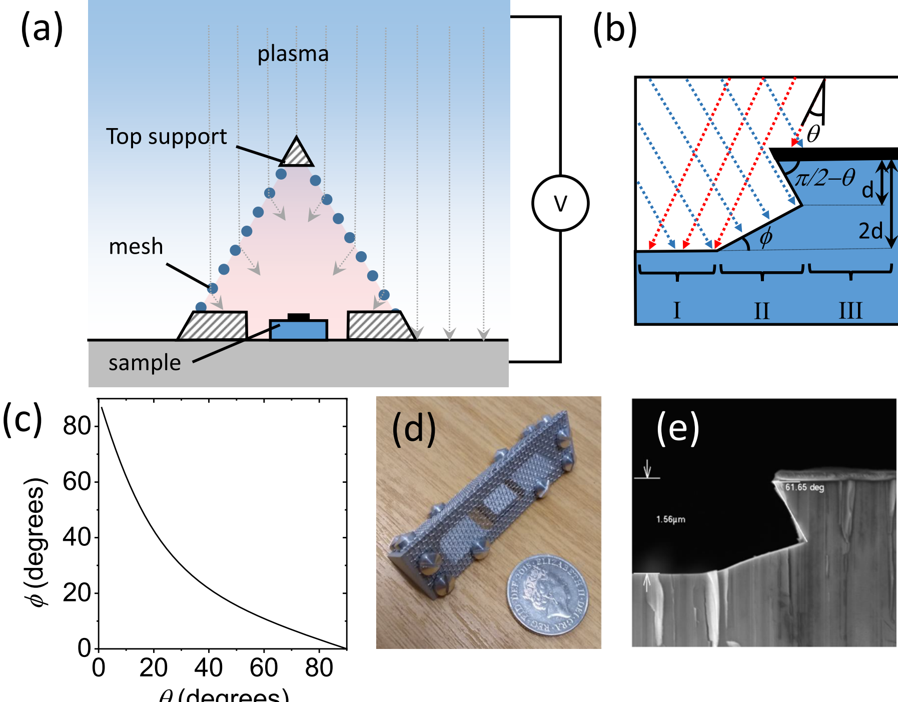

FIG. 1. (a) Schematic of the cross section of the etch chamber containing the Faraday cage, with the GaN samples at its center, (b) schematic showing how ions directed at steep angles θ cause the characteristic undercut profile, (c) the plot of the predicted etch angles ϕ and θ, (d) a photograph of the triangular Faraday cage with a UK ten-pence coin for scale (diameter 24.5 mm), and (e) a scanning electron micrograph of a cleaved edge of a GaN waveguide sample etched in the cage to a depth $2d$ = 1.56 μm.

© Author(s) 2020

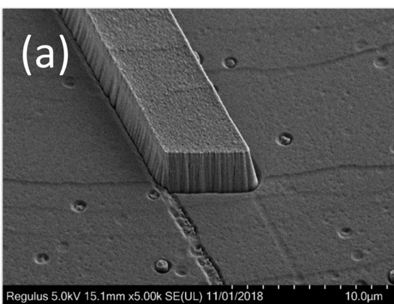

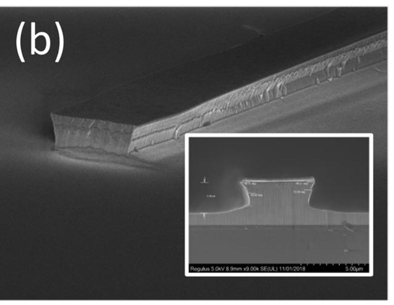

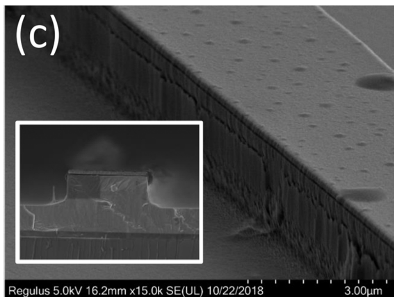

FIG. 2. (a) Stripe etched without the cage, showing an etch angle of −15°, typical of ICP etched GaN, (b) an etch with the sample in a 45° cage and with the same 1:1 Cl_2:Ar gas mix, leading to a −22° etch, and (c) an etch in a 45° cage with a 5:1 Cl_2:Ar mix to give a θ = 0° etch profile.

used to hold the mesh in its place, tend to distort the field and deflect the ions undesirably, creating an uneven etch over the sample surface.

To investigate the optimum conditions for etching, we have carried out a study where we have varied the gas mix in the plasma, bias, and plasma power in addition to changing the angle of the Faraday cage and mesh size. To illustrate some of the main findings, we show in Fig. 2(a) images of a series of stripes etched into c-plane GaN-on-sapphire using nickel as a hard mask, with 200 W plasma power, 10 mT field, and a chlorine–argon gas mix. We use the ratio in which these gases are introduced to the etch chamber to control the relative strength of the physical (anisotropic) and chemical (isotropic) etch for fixed plasma power. As shown in Figs. 2(a) and 2(b), the two gases have equal pressure. In Fig. 2(a), the sample is etched with no cage present, so ions are incident on the semiconductor from the vertical direction, resulting in a cross-sectional profile which is wider at the bottom than the top, with an etch angle of −15°. The irregularities visible on the etched surface are due to dislocations in the GaN crystal. Figure 2(b) shows the same etch process run on an identical chip inside a cage with walls at 45°. We now see the characteristic cross-sectional profile, as illustrated in Fig. 1. Once again, the etch angle θ = 22° is lower than the angle of the cage walls (45°). The etched surface away from the stripe is smoother than that shown in Fig. 2(a), consistent across all samples we have studied. It is outside the scope of this work to quantify the roughness of this surface, but this may be an area of interest for future studies.

Finally, we etched a sample in the same 45° cage with the same total pressure but with a 5:1 Cl_2:Ar gas mix to produce an etch with a stronger chemical character. This gives a cross-sectional profile with vertical sidewalls, θ = 0°, which may be advantageous for the creation of photonic integrated circuits. Thus, even without structural changes to the cage, it is possible to modify the etch angles by changing the gas mix. The greatest angle of etch we have been able to achieve is 40° with this cage. This opens up the possibility of producing more complex etch profiles within a single etch by dynamically changing the gas mix.

Using this cage-assisted etch process, it is possible to create suspended GaN devices in a single step if the etch angle θ, the etch depth d, and the stripe width w meet the condition $2d \tan\theta > w$. A series of samples were prepared with w = 1–2 μm, which were etched in the Faraday cage with an equilateral triangle cross-section to create an etch with θ = 30°, as shown in Fig. 1(c). This suggests that under these conditions, the etch angle is close to half the cage angle for the two cage designs tested. These were etched to a depth of $2d$ = 2.00 μm, creating suspended beams with an equilateral triangular cross section, as shown in Fig. 3. The beams may be clamped either at one end (a) or both ends (b), without collapsing. The residual "foot" of the etch with an angle ϕ is visible beneath the beam and becomes less prominent as the process time is increased. The mechanical stiffness of GaN allows the Ni mask to be removed with nitric acid without the surface tension causing the beams to collapse, as is often reported with suspended GaAs/AlAs devices. This

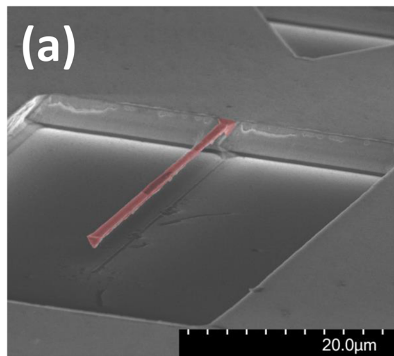

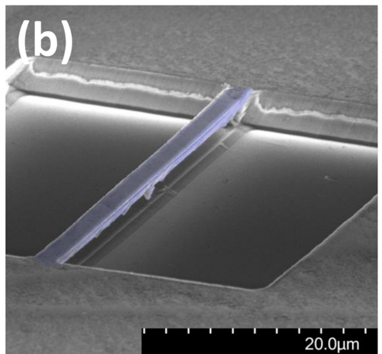

FIG. 3. (a) Free-standing singly clamped triangular cantilever 1 μm in width and 35 μm in length, suspended 2 μm above a planar layer, etched inside a Faraday cage with an equilateral triangular cross section and (b) a suspended doubly-clamped cantilever of 2 μm width.

© Author(s) 2020

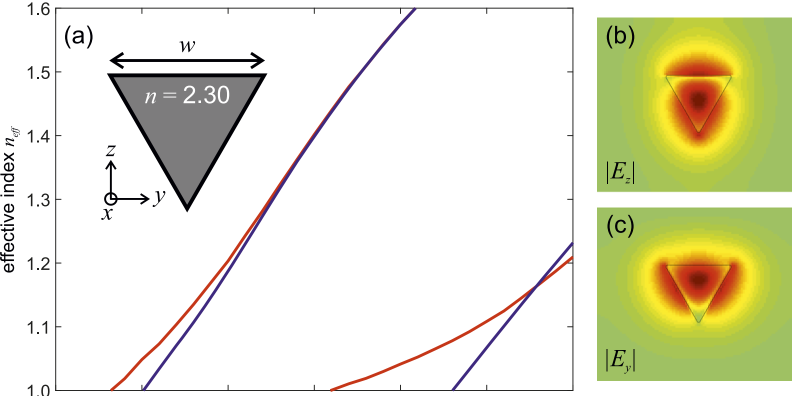

FIG. 4. Calculations of waveguides with an equilateral triangular cross-section: (a) the effective index of the waveguide modes (blue: TE and red: TM) as a function of the waveguide size (inset: the schematic of the calculation) and [(b) and (c)] the mode profiles for (b) the fundamental TE mode and (c) the TM mode.

1-step etch process, therefore, provides a simple method to create cantilevers and suspended MEMS devices similar to those reported in silicon. However, GaN is a particularly stiff material hosting mature light emitting heterostructures and may offer new functionalities for opto-mechanical coupling.

The suspended triangular beams we create here are expected to guide light with confinement provided by the index difference between GaN and the surrounding air or vacuum. We have calculated the optical eigenmodes of waveguides with an equilateral triangular cross section with a side length w and a refractive index n = 2.30, suitable for GaN at a wavelength of λ = 1550 nm [the schematic is the inset in Fig. 4(a)]. Figure 4(a) shows the effective index of the waveguide mode as a function of the triangle size w. For TE polarization, a single mode exists for equilateral triangular widths between w = 500 nm and 850 nm, whereas TM polarization has a single mode between w = 480 nm and 710 nm. Figures 2(b) and 2(c) show the field profiles for the fundamental (and only) mode for triangular waveguides with a width w = 700 nm. The modes are highly confined to the waveguide core. Although the angled etch is essential to create a suspended structure, it may not be optimal for the optical performance of a waveguide, which will be the focus of future work.

In conclusion, we have presented a Faraday cage-assisted process to etch GaN with a controlled angle of undercut. We have shown that by adjusting the gas mix in the ICP chamber, it is possible to vary the etch angle without changing the cage design. We have created suspended GaN nano-cantilevers with a triangular cross section. Simulations show that these can support single optical modes in the near infrared, with potential for integrated photonics that exploits the advantageous optical properties of GaN. Future work may focus on the creation of 1D photonic crystals in suspended GaN devices. It is also possible to consider alternative designs of the Faraday cage, such as conical cages, to create undercut devices with a cylindrical symmetry.

We acknowledge funding from the Engineering and Physical Sciences Research Council Grant Nos. EP/P006973/1 and EP/T017813/1. We thank Bedwyr Humphreys for useful advice and Paul Leach for assisting us with the manufacturing of the Faraday cage.

DATA AVAILABILITY

The data that support the findings of this study are openly available in the Cardiff University data catalogue at http://doi.org/10.17035/d.2020.0108194561.

REFERENCES

[1] P. Middlemiss, A. Samarelli, D. J. Paul, J. Hough, S. Rowan, and G. D. Hammond, Nature **531**, 614–617 (2016).
[2] J. Chan *et al.*, Nature **478**, 89–92 (2011).
[3] J. C. Adcock, C. Vigliar, R. Santagati, J. W. Silverstone, and M. G. Thompson, Nat. Commun. **10**, 3528 (2019).
[4] K. Hennessy, A. Badolato, M. Winger, D. Gerace, M. Atatüre, S. Gulde, S. Fält, E. L. Hu, and A. Imamoğlu, Nature **445**, 896–899 (2007).
[5] A. Javadi *et al.*, Nat. Nanotechnol. **13**, 398–403 (2018).
[6] C. P. Dietrich, A. Fiore, M. G. Thompson, M. Kamp, and S. Höfling, Laser Photonics Rev. **10**, 870–876 (2016).
[7] T. Zhong *et al.*, Phys. Rev. Lett. **121**, 183603 (2018).
[8] A. J. Steckl and I. Chyr, J. Vac. Sci. Technol., B **17**, 362 (1999).
[9] G. D. Boyd, L. A. Coldren, and F. G. Storz, Appl. Phys. Lett. **36**, 583 (1980).
[10] T. Takamori, L. A. Coldren, and J. L. Merz, Appl. Phys. Lett. **53**, 2549 (1988).
[11] J.-K. Lee, S.-H. Lee, J.-H. Min, I.-Y. Jang, C.-K. Kim, and S. H. Moon, J. Electrochem. Soc. **156**, D222 (2009).
[12] M. J. Burek, Y. Chu, M. S. Z. Liddy, P. Patel, J. Rochman, S. Meesala, W. Hong, Q. Quan, M. D. Lukin, and M. Lončar, Nat. Commun. **5**, 5718 (2014).
[13] P. Latawiec, M. J. Burek, Y.-I. Sohn, and M. Lončar, J. Vac. Sci. Technol., B **34**, 041801 (2016).
[14] M. Kang, C. Lee, J. Park, H. Yoo, and G. Yia, Nano Energy **1**, 391–400 (2012).
[15] T. Zhu and R. A. Oliver, Europhys. Lett. **113**(3), 38001 (2016).
[16] A. M. Berhane *et al.*, Adv. Mater. **29**, 1605092 (2017).
[17] C. Xiong, W. Pernice, K. K. Ryu, C. Schuck, K. Y. Fong, T. Palacios, and H. X. Tang, Opt. Express **19**(11), 10462–10470 (2011).
[18] N. Niu, A. Woolf, D. Wang, T. Zhu, Q. Quan, R. A. Oliver, and E. L. Hu, Appl. Phys. Lett. **106**, 231104 (2015).
[19] S. Jagsch, N. Vico Triviño, F. Lohof, G. Callsen, S. Kalinowski, R. Barzel, J. Carlin, F. Jahnke, R. Butté, C. Gies, A. Hoffmann, N. Granjean, and S. Reitzenstein, Nat. Commun. **9**, 564 (2018).
[20] R. Butté and N. Grandjean, Nanophotonics **9**(3), 569–598 (2020).
[21] N. Vico Triviño, G. Rossbach, U. Dharanipathy, J. Levrat, A. Castiglia, J.-F. Carlin, K. A. Atlasov, R. Butté, R. Houdré, and N. Grandjean, Appl. Phys. Lett. **100**, 071103 (2012).
[22] I. Roland *et al.*, Appl. Phys. Lett. **105**, 011104 (2014).

© Author(s) 2020